

SLAC - PUB - 5118
20 October 1989
(T/E)

**Recent Results on Weak Decays of Charmed Mesons
from the MarkIII experiment***

Thomas E. Browder

Stanford Linear Accelerator Center, Stanford, CA, 94309.
and Cornell University, Ithaca, New York, 14853.

Recent results from the MarkIII experiment on weak decays of charmed mesons are presented. Measurements of the resonant substructure of $D^0 \rightarrow K^- \pi^+ \pi^- \pi^+$ decays, the first model independent result on $D_s \rightarrow \phi \pi^+$, as well as limits on $D_s \rightarrow \eta \pi^+$ and $D_s \rightarrow \eta' \pi^+$ are described. The implications of these new results are also discussed.

Invited Talk at the 17th SLAC Summer Institute:

Physics at the 100 GeV Mass Scale, Stanford, CA. July 10-21, 1989.

* Work supported by Department of Energy Contract DE-AC-03-76SF00515

Resonant Substructure in $D \rightarrow K\pi\pi\pi$ Decays

A number of $D \rightarrow PP$ and $D \rightarrow PV$ decays^[1] have now been measured and can be satisfactorily explained in two phenomenological models.^[2] So far these models have not been tested for the case of $D \rightarrow VV$ decays. Using the decay mode $D^0 \rightarrow K^- \pi^+ \pi^- \pi^+$ the branching ratio for $D^0 \rightarrow \bar{K}^{*0} \rho^0$ can be determined. In addition to the possibility of measuring the VV components, it is also important to measure the resonant subcomponents of $D \rightarrow K\pi\pi\pi$ decays since these decays comprise a significant fraction of the total D width [35% of the D^0 width and 20% of the D^+ width].

Using the data sample [9.3 pb⁻¹] collected at the $\psi''(3.77)$ between 1982 and 1984, a complete resonant substructure analysis has been carried out for the decay modes $D^0 \rightarrow K^- \pi^+ \pi^- \pi^+$ and $D^+ \rightarrow \bar{K}^0 \pi^- \pi^+ \pi^+$ by the MarkIII group.^[3] A large clean signal for the all charged mode is shown in the recoil mass plot of Figure 1(a). The fitted signal contains 1281 ± 45 events. An equally clean signal, with 184 ± 21 events, for $D^+ \rightarrow \bar{K}^0 \pi^+ \pi^- \pi^+$ is shown in Figure 1(b).

An unbinned maximum likelihood fit to the full five dimensional phase space defined by the four momenta of the D decay products is performed in order to determine the resonant content of the decay mode. A set of amplitudes which describe the resonant substructure of the decay is chosen. The preferred fit for the mode $D^0 \rightarrow K^- \pi^+ \pi^- \pi^+$ includes contributions from $D^0 \rightarrow K^- \pi^+ \pi^- \pi^+$ in a non-resonant state, $D^0 \rightarrow \bar{K}^{*0} \pi^- \pi^+$, $D^0 \rightarrow K^- \rho^0 \pi^+$, $D^0 \rightarrow K^- a_1^+(1260)$, $D^0 \rightarrow K_1(1270)^- \pi^+$, $D^0 \rightarrow K_1(1400)^- \pi^+$, and $D^0 \rightarrow \bar{K}^{*0} \rho^0$. The $D^0 \rightarrow \bar{K}^{*0} \rho^0$ term contains two independent components in which either both vector mesons are polarized parallel or both vector mesons are polarized perpendicular to the direction of flight of the D^0 meson.

The amplitude for each of the above processes is expressed in terms of two body masses using the Lorentz invariant amplitude formalism or in terms of helicity angles using the helicity formalism. The amplitudes are symmetrized with respect to the labels of identical pions. The amplitudes so obtained are

then multiplied by relativistic Breit Wigners and modulated by form factors. All the amplitudes are fully interfering. A Monte Carlo integration technique is used to take account of the dependence on detector acceptance and avoid the problem of parameterizing the acceptance in the five dimensional phase space.

The sidebands in recoil mass are used to determine the background likelihood function. The likelihood function allows for non-resonant, $K^{\bar{*}0}$, ρ^0 , and $K^{\bar{*}0}\rho^0$ components in the background. These components are non-interfering.

The possibility that the choice of amplitudes may introduce some model dependence is one of the difficult issues that must be addressed in this analysis. A large number of decay modes could potentially contribute to the $D^0 \rightarrow K^- \pi^+ \pi^- \pi^+$ final state. It is not practical to perform a fit that simultaneously includes all the possibilities. Instead, a large number of fits with different combinations of amplitudes were performed. Those fits which yielded a good likelihood were retained for further consideration. Fits which were physically implausible were discarded. The final set of fits give similar results for the quasi two body amplitudes and for the four body non-resonant amplitude. The fits did not yield definitive results on which quasi three body partial waves contribute. The range of variation among the final set of fits is used to estimate the systematic error.^[4]

Since the a_1 is very broad, it is often difficult to distinguish it from non-resonant $\rho^0\pi$. The polarization of $D^0 \rightarrow K^- a_1 [P \rightarrow P A]$ leads to angular distributions which are distinctive. However, $D^0 \rightarrow K^- a_1$ cannot be separated from the reaction $D^0 \rightarrow K^- \rho^0 \pi^+$ where the ρ^0 and π^+ are in relative s wave on the basis of angular information. The three pion mass distributions for these two possibilities are, however, significantly different; the $D^0 \rightarrow K^- a_1$ amplitude peaks about 100 MeV above the nonresonant amplitude. Fits in which the Ka_1 amplitude was replaced by the three body amplitude resulted in a significantly smaller likelihood, with a difference in $\ln(L)$ of at least 12. Therefore it is assumed that this particular three body amplitude does not contribute to the final states discussed here.

Projections of the five dimensional likelihood function for various submasses are shown in Figure 2. A large K^* contribution is evident in Figure 2(a). Similarly, ρ production is evident in Figure 2(b). The enhancement at low $K^-\pi^-$ mass in Figure 2(e) is due to the polarization of the a_1 . Evidence for $D^0 \rightarrow K_1(1270)\pi^+$ is visible in Figure 2(g). In all the projections the fit is in good agreement with the data.

Table I Preliminary results for $D^0 \rightarrow K^-\pi^-\pi^+\pi^-\pi^+$

Amplitude	Fraction	Phase	Branching Ratio
4-Body Nonresonant	$.233 \pm .025 \pm .10$	$-1.01 \pm .08$	$.021 \pm .003 \pm .009$
$\bar{K}^{*0}\rho^0$ Longitudinal	$.014 \pm .009 \pm .01$	$-2.64 \pm .28$	Sum of L and T:
$\bar{K}^{*0}\rho^0$ Transverse	$.152 \pm .021 \pm .05$	$-1.22 \pm .11$	$.023 \pm .003 \pm .007$
$K^-a_1(1260)$	$.442 \pm .021 \pm .10$.0	$.080 \pm .008 \pm .019$
$K_1(1270)^-\pi^+$	$.113 \pm .028 \pm .04$	$.44 \pm .19$	$.031 \pm .008 \pm .011$
$K_1(1400)\pi^+$	$.011 \pm .009 \pm .03$	$.71 \pm .43$	< .012
$K^{*0}\pi^+\pi^-$	$.091 \pm .018 \pm .04$	$-3.31 \pm .11$	$.012 \pm .003 \pm .005$
$K^-\rho^0\pi^+$	$.088 \pm .023 \pm .04$	$-.62 \pm .09$	$.008 \pm .002 \pm .004$

The results of the fit are shown in Table I. A few qualitative features should be noted. There is a very large $D^0 \rightarrow K^-a_1(1260)$ [$D \rightarrow P A$] contribution to this final state, consistent with the theoretical expectation from the BSW model [5.0%]. There is also a rather small $D^0 \rightarrow \bar{K}^{*0}\rho^0$ [$D \rightarrow V V$] contribution, which is completely polarized transverse to the D^0 flight direction. There is some evidence for the final state $D^0 \rightarrow K_1(1270)^-\pi^+$ [$D \rightarrow A P$]. The four body non-resonant contribution is also significant. In addition, there is a contribution from $D^0 \rightarrow \bar{K}^{*0}\pi^-\pi^+$ where the $\bar{K}^{*0}\pi^+$ system is in an axial vector state as well as $D^0 \rightarrow K^-\rho^0\pi^+$ where the $K^-\rho^0$ system is an axial vector state. It is not possible to determine whether the above three body amplitudes are due to quasi two body decays of broad resonances e.g. $D^0 \rightarrow K^-\pi(1300)^+$ or $D^0 \rightarrow K(1460)^-\pi^+$.

An analysis for the mode $D^+ \rightarrow \bar{K}^0\pi^-\pi^+\pi^-$ has been carried out using the same technique. The results of the fit are shown in Table II. There is a large

contribution from the axial-vector pseudoscalar mode $D^+ \rightarrow \bar{K}^0 a_1(1260)^+$. There is also some evidence for $D^+ \rightarrow K_1(1400)\pi^+$ [$D \rightarrow A P$]. There is no possible vector vector mode that can contribute to this final state.

Table II Results for $D^+ \rightarrow \bar{K}^0 \pi^- \pi^- \pi^+$

Amplitude	Fraction	Phase	Branching Ratio
4-Body Nonresonant	$.184 \pm .052 \pm .10$	$1.37 \pm .17$	$.012 \pm .004 \pm .007$
$\bar{K}^0 a_1(1260)^+$	$.612 \pm .053 \pm .15$.0	$.081 \pm .020 \pm .027$
$K_1(1270)\pi^+$	$.010 \pm .013 \pm .02$	$1.30 \pm .90$	$< .011$
$K_1(1400)\pi^+$	$.163 \pm .048 \pm .08$	$.24 \pm .26$	$.024 \pm .009 \pm .013$

Resonant substructure analyses of the modes $D^0 \rightarrow K^- \pi^+ \pi^0 \pi^0$, $D^+ \rightarrow K^- \pi^+ \pi^+ \pi^0$, and $D^0 \rightarrow \bar{K}^0 \pi^- \pi^+ \pi^0$ channels will also be attempted in the near future. If the rates and phases for $D^0 \rightarrow \bar{K}^{*0} \rho^0$, $D^0 \rightarrow \bar{K}^{*-} \rho^+$, and $D^+ \rightarrow \bar{K}^{*0} \rho^+$ can be measured with sufficient accuracy, then the isospin sum rule^[6]

$$\sqrt{2}A(D^0 \rightarrow \bar{K}^{*0} \rho^0) = A(D^+ \rightarrow \bar{K}^{*0} \rho^+) - A(D^0 \rightarrow \bar{K}^{*-} \rho^+)$$

can be used to determine whether final state interactions play a significant role in these decays. If the above sum rule cannot be satisfied with relatively real amplitudes, then final state interactions are required. Examination of the other final states will also provide good consistency checks of the resonant substructure analysis since quasi two body reactions can give rise to several distinct final states e.g. $D^0 \rightarrow \bar{K}^{*0} \rho^0 \rightarrow K^- \pi^+ \pi^- \pi^+$ or $\bar{K}^0 \pi^0 \pi^- \pi^+$.

In addition to measurements of the absolute rates of $D \rightarrow V V$ decays, it is also possible to measure angular correlations between the two vectors in $D \rightarrow V V$ decays. This is useful for testing the factorization hypothesis.^[6] If the two vectors are both polarized perpendicular to the D^0 direction, one expects that the angular dependence of the amplitude will have the form $A_T \propto \cos(\phi) \sin \theta_1 \sin \theta_2$ where ϕ is the angle between the decay planes of the two vector mesons, and θ_1 ,

θ_2 are the helicity angles of the ρ and K^* mesons, respectively. If the polarization is longitudinal, $A_L \propto \cos \theta_1 \cos \theta_2$. If factorization is a valid assumption, longitudinal polarization is expected to be dominant. The analysis by the MarkIII group, however, indicates that $D^0 \rightarrow \bar{K}^{*0} \rho^0$ is transversely polarized. The observed angular correlation for $D^0 \rightarrow \bar{K}^{*0} \rho^0$ events is indicated in Figure 3.

Several recent observations appear to indicate that many of the VV decay rates are smaller than expected. For instance, the measured rate for $D^0 \rightarrow \bar{K}^{*0} \rho$ ($2.3 \pm 0.3 \pm 0.7\%$) from MarkIII is almost three times smaller than the theoretical expectation (6.1%). The branching ratio for the decay $D_s \rightarrow \phi \pi^+ \pi^0$, which is expected to include a large $\phi \rho^+$ contribution, is $2.4 \times \text{Br}(D_s \rightarrow \phi \pi^+)$, nearly a factor of three smaller than the prediction [$6.3 \times \text{Br}(D_s \rightarrow \phi \pi)$]. Similarly, even if the decay $D^+ \rightarrow K^- \pi^+ \pi^+ \pi^0$ is saturated by $D^+ \rightarrow \bar{K}^{*0} \rho^+$, the observed rate^[7] [$3.7 \pm 0.8 \pm 0.8\% / \text{Br}(K^{*0} \rightarrow K^- \pi^+)$] is still significantly lower than the BSW prediction [$\sim 13\%$]. These intriguing discrepancies may indicate the breakdown of the factorization Ansatz in decays with little energy release.^[8] If the same models are used to extract information about the weak interaction in B decays, it is necessary to understand why these phenomenological models fail in the case of $D \rightarrow V V$.

The Absolute Branching Fraction $B(D_s \rightarrow \phi \pi^+)$

All D_s decay measurements are normalized to $B(D_s \rightarrow \phi \pi^+)$. In addition, to extract $B(B \rightarrow D_s X_i)$ from a measurement of $B \rightarrow D_s X_i \rightarrow \phi \pi X_i$ for a final state X_i requires knowledge of the absolute branching fraction $B(D_s \rightarrow \phi \pi^+)$.^[9]

There are three methods that can be used to extract the absolute branching fraction. For the majority of published results, one uses the measured quantity $\sigma_{D_s} \times \text{Br}(D_s \rightarrow \phi \pi^+)$ for $x_{D_s} > \text{cut}$ where $x_{D_s} = p(D_s)/p_{max}$. The measured D_s yield is extrapolated to all x_{D_s} using a model for the D_s fragmentation function. A theoretical value of σ_{D_s} is then calculated and the absolute branching fraction is determined. The theoretical value of σ_{D_s} depends on the probability of popping an s sbar quark pair from the vacuum and is sensitive to the details of D_s

hadronization. The results obtained using this method range from 1.7% to 4.4%.

[10-20]

A second method based on charm counting has been used recently as well. From the measured value of R in the continuum above the resonance region, the total charm cross section is inferred from the quark charges. The total charm cross section can then be decomposed into the following components:

$$\sigma_{\text{charm}} = \sigma_{D^0} + \sigma_{D^+} + \sigma_{D_s} + \sigma_{\Lambda_c} + \sigma_{\text{other baryons}}.$$

If the last term on the right hand side can be absorbed into the other terms, then

$$\sigma_{D_s} = \sigma_{\text{charm}} - \sigma_{D^0} - \sigma_{D^+} - \sigma_{\Lambda_c}.$$

The cross section σ_{D^0} is obtained by dividing the observed quantity $\sigma_{D^0} \times Br(D^0 \rightarrow f_i)$ by the absolute branching fraction $Br(D^0 \rightarrow f_i)$ from MarkIII. The final states $f_i = K^- \pi^+$ and $K^- \pi^+ \pi^- \pi^+$ are used. The cross section σ_{D^+} is obtained in a similar way using the final state $D^+ \rightarrow K^- \pi^+ \pi^+$. The cross section σ_{Λ_c} is determined from the measured Λ_c yield and the branching fraction for $\Lambda_c \rightarrow p K^- \pi^+$. The Λ_c branching fraction is in turn determined either from the measured $B \rightarrow \text{proton X}$ rate or from the MarkII continuum measurement. Using these cross sections, the absolute branching fraction is determined by the CLEO collaboration to be $2 \pm 1\%$.^[21] This result is sensitive to the Λ_c branching fraction and assumptions about charmed baryon production.

The third method, which is used by the MarkIII experiment, employs the reaction $e^+ e^- \rightarrow D_s^\pm D_s^{*\mp}$ decays where the full final state is completely reconstructed. This method was successfully used to extract absolute D^0 and D^+ branching fractions from the data sample collected at the $\psi(3.77)''$ resonance.^[22]

The principle and advantages of this double tagging technique method are easy to understand. The number of double tags with $D_s \rightarrow f_i$ opposite $D_s \rightarrow \phi \pi$

will be given by

$$2\sigma_{D_s D_s}; L B(D_s \rightarrow f_i) B(D_s \rightarrow \phi\pi) \epsilon_{f_i} \epsilon_{\phi\pi}.$$

The number of singly tagged $D_s \rightarrow f_i$ events will be given by

$$\sigma_{D_s D_s}; L B(D_s \rightarrow f_i) \epsilon_{f_i}.$$

Therefore

$$N_{double}/(2N_{single}\epsilon_{\phi\pi}) = B(D_s \rightarrow \phi\pi^+)$$

This result is manifestly model independent. Clearly, the above derivation can easily be extended to any doubly tagged decay modes [f_i versus f_j] provided the branching ratios of $B(D_s \rightarrow f_i)$ and $B(D_s \rightarrow f_j)$ are known relative to $B(D_s \rightarrow \phi\pi^+)$.

The MarkIII analysis^[23] is performed using the data sample [6.3 pb⁻¹] collected in 1986 at $\sqrt{s} = 4.14$ GeV. Candidates for the reaction $e^+e^- \rightarrow D_s^\pm D_s^{*\mp}$, $D_s^+ \rightarrow f_i$, $D_s^{*-} \rightarrow \gamma D_s^-$, $D_s^- \rightarrow f_j$ are selected using a six constraint kinematic fit. Energy momentum conservation for the exclusive final state leads to four constraints. The additional two constraints are due to the equal mass requirement $m(f_i) = m(f_j) = m(X)$ i.e. the two D_s candidates must have equal but unspecified masses. Candidates for the decay modes $D_s \rightarrow \phi\pi^+$, $D_s \rightarrow \bar{K}^0 K^+$, $D_s \rightarrow K^{*0} K^+$, $D_s \rightarrow f_0(975)\pi^+$, $D_s \rightarrow \phi\pi^+\pi^-\pi^+$, $D_s \rightarrow \phi\pi^+\pi^0$, and $D_s \rightarrow K^{*0} K^{*+}$ are considered. There are a total of 28 possible final states.

A signal region which contains 95% of the signal events is determined for each of the combinations on the basis of Monte Carlo simulation. The observed $M(X)$ distribution is the unshaded histogram in Figure 4(a). The expected $M(X)$ distribution is the histogram shown in Figure 4(b). The arrows indicate the limits of the signal region for the combination of modes with the poorest resolution [± 20 MeV]. There are no candidate events inside the signal region. If $B(D_s \rightarrow \phi\pi^+) = 4\%$, we should observe 3 events in the signal region.

A likelihood function which depends on the $D_s \rightarrow \phi\pi^+$ branching ratio is used to obtain the upper limit. The likelihood function is integrated to obtain the 90% confidence level upper limit. After allowing for systematic error in the detection efficiency and gaussian errors on the relative branching fractions of the tagging modes, the upper limit $B(D_s \rightarrow \phi\pi^+) < 4.1\%$ at the 90% confidence level is obtained.^[24]

Search for D_s Decays to $\eta\pi$ and $\eta'\pi^+$ Final States.

If the absolute branching fraction $B(D_s \rightarrow \phi\pi) \sim 2\%$ then only $9 \times B(D_s \rightarrow \phi\pi)$ or 18% of all hadronic D_s decays have been measured. The existing measurements of D_s modes are summarized in Tables II and III. It has been suggested that $D_s \rightarrow \eta\pi$ and $D_s \rightarrow \eta'\pi$ could account for a large fraction of the missing D_s modes. Two recent results from the MarkII^[25] and NA14^[26] experiments appear to confirm this suggestion. Clearly, it is important to provide a definitive experimental resolution of this issue.

Due to these surprising observations, there has been a great deal of theoretical interest in these D_s decay modes. The decay $D_s \rightarrow \eta\pi^+$ is expected to proceed via a spectator diagram and should therefore be comparable in rate to $D_s \rightarrow \phi\pi^+$. Predictions are available from Bauer, Stech and Wirbel(BSW)^[27], Korner and Schuler(KS)^[28], and Blok and Shifman(BS).^[29] They find that $D_s \rightarrow \eta\pi^+ / D_s \rightarrow \phi\pi^+$ should be 0.75 – 1.05(BSW), 1.35 – 1.89(KS), or 1.1(BS). The ratio of $B(D_s \rightarrow \eta'\pi^+) / B(D_s \rightarrow \eta\pi^+)$ is determined primarily by the s sbar quark content of the η and η' mesons, and by the amount of available phase space. Since the η' is more massive than η and has much less s sbar quark content, one expects naively: $B(D_s \rightarrow \eta'\pi^+) / B(D_s \rightarrow \eta\pi^+) < 1$. For this ratio, BSW predict 0.59 – 1.04, while KS predict 0.62 – 1.09. Blok and Shifman find 0.09. The range of the theoretical predictions in the first two cases is due to the possible choices of the $\eta - \eta'$ mixing angle (the two canonical choices are $\theta_p = 11$ or 19 degrees). The difference between the BSW and KS predictions is due to the method used for

Table 3. Branching Ratios of D_s modes with kaons relative to $\phi\pi$

Decay Mode	Experiment	Result or Limit
$D_s \rightarrow \bar{K}^0 K^+$	MarkIII	$0.92 \pm 0.32 \pm 0.20$
	CLEO	$0.99 \pm 0.17 \pm 0.06$
$D_s \rightarrow \bar{K}^{*+} K^0$	CLEO	$1.2 \pm 0.21 \pm 0.07$
$D_s \rightarrow \bar{K}^0 \pi^+$	MarkIII	< 0.21 at 90% CL
$D_s \rightarrow \bar{K}^{*0} K^+$	E691	$0.87 \pm 0.13 \pm 0.05$
	ARGUS	1.44 ± 0.37
	MarkIII	$0.84 \pm 0.30 \pm 0.22$
	CLEO	$1.05 \pm 0.17 \pm 0.06$
$D_s \rightarrow \bar{K}^{*0} K^{*+}$	NA32	2.3 ± 1.2
$D_s \rightarrow \phi \pi^+ \pi^0$	E691	$2.4 \pm 1.0 \pm 0.5$
	NA14	< 2.6 at 90% CL
$D_s \rightarrow (K^- K^+ \pi^+)_{NR}$	E691	$0.25 \pm .07 \pm .05$
	NA32	0.96 ± 0.32
$D_s \rightarrow \phi \pi^- \pi^+ \pi^+$	E691	$0.42 \pm 0.13 \pm .07$
	NA32	0.39 ± 0.17
	Argus(a)	$1.11 \pm 0.37 \pm 0.28$
	Argus(b)	$0.41 \pm 0.13 \pm 0.11$
$D_s \rightarrow (K^- K^+ \pi^+ \pi^0)_{NR}$	E691	< 2.4 at 90% CL
$D_s \rightarrow (K^- K^+ \pi^- \pi^+ \pi^+)_{NR}$	E691	$< .32$ at 90% CL
	NA32	0.11 ± 0.07

determining the hadronic form factors; BSW use relativistic harmonic oscillator wave functions to calculate the meson overlaps while KS use SU(4) symmetry.

In addition to the predictions listed above, Kamal and Sinha^[80] have attempted a coupled channel treatment with three rescattering modes but were also unable to reproduce the large rates reported by MarkII and other experiments. Moreover, they note that the large ratio $D_s \rightarrow \eta' \pi^+ / D_s \rightarrow \eta \pi^+ \sim 2$ cannot be accommodated within the standard range of $\eta - \eta'$ mixing for either a 10 or 19 degree pseudoscalar mixing angle. They claim that neither decay mode can be significantly enhanced by annihilation diagrams or penguins. The large rate

Table 4. Branching Ratios of D_s modes without kaons relative to $\phi\pi$

Decay Mode	Experiment	Result or Limit
$D_s \rightarrow \rho\pi^+$	E691	< 0.08 at 90% C.L.
	Argus	< 0.22 at 90% C.L.
$D_s \rightarrow f_0(975)\pi^+$	E691	$0.28 \pm 0.1 \pm .03$
	MarkIII	$0.58 \pm 0.21 \pm 0.28$
$D_s \rightarrow \eta\pi^+$	E691	< 1.5 at 90% CL
	MarkII	3.0 ± 1.1
	MarkIII	< 2.5 at 90% CL
$D_s \rightarrow \eta'\pi^+$	MarkII	4.8 ± 2.1
	NA14	$6.9 \pm 2.4 \pm 1.4$
	MarkIII	< 1.9 at 90% CL
	E691	< 1.7 at 90% CL
$D_s \rightarrow \omega\pi^+$	E691	< 0.5 at 90% CL
	E564	seen
$D_s \rightarrow (\pi^-\pi^+\pi^+)_{NR}$	E691	$0.29 \pm .09 \pm .03$
$D_s \rightarrow (\pi^-\pi^+\pi^+\pi^-\pi^+)_{NR}$	E691	$< .29$ at 90% CL

for η modes, they speculate, is due to the presence of the decay $D_s \rightarrow \text{glue } \pi^+$ or some other unconventional process. In contrast to Kamal and Sinha, L.L Chau concludes that the rates for $D_s \rightarrow \eta\pi^+, \eta'\pi^+$ demonstrate that annihilation is large in D_s decays.^[31]

In a complementary approach using SU(3) flavor symmetry constraints, Rosen^[32] derives the inequality $Br(D_s \rightarrow \eta\pi^+) < 9\%$ given the canonical choice $\theta_p = 19^\circ$ (or $Br(D_s \rightarrow \eta\pi^+) < 5.3\%$ for $\theta_p = 10^\circ$). He also finds that the ratio $Br(D_s \rightarrow \eta'\pi^+)/Br(D_s \rightarrow \eta\pi^+) < 0.22(0.43)$ for $\theta_p = 20^\circ$ (10°). The large rates reported for the two reactions therefore indicate substantial SU(3) breaking effects.

The data sample collected at 4.14 GeV is used for the MarkIII analysis of $D_s \rightarrow \eta\pi^+$ and $D_s \rightarrow \eta'\pi^+$. The barrel and endcap shower counters are used

to identify photon candidates. The MarkIII shower counter has a resolution $\sigma(E)/E = 18\%/\sqrt{E}$. The shower counter efficiency is 100% for photons with energies above 0.1 GeV. Both TOF and energy loss (dE/dx) information are used to identify charged pions.

In the analysis of the decay sequence $D_s \rightarrow \eta\pi^+$, $\eta \rightarrow \pi^+\pi^-\pi^0$, candidate π^0 's are selected by performing a 1-C kinematic fit of all pairs of $\gamma\gamma$ candidates to the π^0 mass. Pairs for which the fit chisquared confidence level (CL) is greater than 5% are retained for further consideration. The lower momentum pions from the η decay must be identified as pions. A 2-C kinematic fit to the hypothesis $e^+e^- \rightarrow \pi^+\pi^-\pi^0\pi^\pm D_s^{*\mp}$, $\pi^0 \rightarrow \gamma\gamma$ is then performed, using all combinations of three pion candidate tracks. The two constraints in the fit are the π^0 mass and the mass of the unobserved $D_s^{*\mp}$. After imposing the requirements $CL > 5\%$ for the 2-C fit, $E_{\text{fit}}^\gamma > 70$ MeV for the photons from the π^0 , and $534 < M(\pi^+\pi^-\pi^0) < 564$ MeV, the $\eta\pi^+$ mass spectrum, shown in Figure 5(a) is obtained. The number of observed $D_s \rightarrow \eta\pi^+$ decays (16.6 ± 6.1) is determined by fitting the resulting mass spectrum. The signal shape is determined from a Monte Carlo simulation. The background shape is determined from the $\pi^+\pi^-\pi^0\pi^\pm$ mass distribution obtained when $M(\pi^+\pi^-\pi^0)$ is selected from the sideband region 0.5738 to 0.6038 GeV. After correcting for the detection efficiency (12.7%) and for the $\eta \rightarrow \pi^+\pi^-\pi^0$ branching ratio, this excess corresponds to $B(D_s \rightarrow \eta\pi^+)/B(D_s \rightarrow \phi\pi^+) = 1.7 \pm 0.7 \pm 0.6 < 3.3$ where the limits are calculated at the 90% confidence level. The estimate of the systematic error includes the uncertainties in the background shape (18%), the detection efficiency (13%), and the integrated luminosity (7%).

In the analysis of the decay sequence $D_s \rightarrow \eta\pi^+$, $\eta \rightarrow \gamma\gamma$, candidate η 's are selected by performing a 1-C kinematic fit of all pairs of $\gamma\gamma$ candidates to the η mass. Pairs for which $CL > 20\%$ are retained. No particle identification is used. A 2-C kinematic fit to the hypothesis $e^+e^- \rightarrow \eta\pi^\pm D_s^{*\mp}$, $\eta \rightarrow \gamma\gamma$ is then performed. In order to reduce combinatorial background, more stringent requirements are imposed than in the preceding analysis: $CL > 10\%$ for the 2-C fit, $E_\gamma^{\text{hi}} > 0.5$ GeV

and $E_\gamma^{\text{lo}} > 0.2$ GeV. When the resulting $\eta\pi^+$ mass distribution, shown in Figure 6(a) is fitted, no evidence for a D_s^+ signal is found. The signal shape is determined from a Monte Carlo simulation. The background shape is a second order polynomial. No sideband region is available since the two photons were constrained to the η mass. The resulting limit, obtained using a detection efficiency of 23.6%, a trigger efficiency of $92 \pm 4\%$, the $\eta \rightarrow \gamma\gamma$ branching ratio and allowing for systematic error (27%), is, $B(D_s \rightarrow \eta\pi^+) / B(D_s \rightarrow \phi\pi^+) < 1.6$ (90% C.L.). The estimate of the systematic error includes the uncertainties in the background shape (20%), the detection efficiency (16%), the trigger efficiency (5%), and the integrated luminosity (7%).

The sensitivity of the two analyses is determined by the product of the detection efficiency and η branching ratios as well as the background levels. In this case, the sensitivity of the two methods are comparable. To combine the results from the two modes properly, a joint likelihood function which depends on the number of produced events is calculated. The joint likelihood function is integrated to determine the 90% confidence level upper limit on the number of produced events, $N_{\eta\pi} < 825$. This yields:

$$\sigma \cdot B(D_s \rightarrow \eta\pi^+) < 66 \text{ pb} \quad (90\% \text{ C.L.})$$

$$\frac{B(D_s \rightarrow \eta\pi)}{B(D_s \rightarrow \phi\pi)} < 2.5 \quad (90\% \text{ C.L.})$$

The analysis presented here uses improved detector constants, fitting techniques, and background simulation than was previously used by the MARKIII in a preliminary analysis of this channel.^[33]

The $\eta'\pi^+$ analysis uses the decay chain, $D_s \rightarrow \eta'\pi^+$, $\eta' \rightarrow \eta\pi^+\pi^-$, $\eta \rightarrow \gamma\gamma$. Photon candidates are selected with a 1-C fit to the η mass, requiring $CL > 10\%$. The low momentum pions from the η' decay are required to be identified as pions. A 2-C kinematic fit to the hypothesis $e^+e^- \rightarrow \eta\pi^+\pi^-\pi^\pm D_s^{*\mp}$, $\eta \rightarrow \gamma\gamma$

is performed, where the masses of the η and the missing $D_s^{*\mp}$ are fixed. After imposing the requirements $E_\gamma^{\text{fit}} > 0.15$ GeV, $\text{CL} > 10\%$ for the 2-C fit, and $|m(\eta\pi^+\pi^-) - m_{\eta'}| < 0.015$ GeV, the $\eta'\pi^+$ mass spectrum, shown in Figure 7 is obtained. The distribution is fitted using a background shape determined from sideband regions 0.922 to 0.937 and 0.977 to 0.992 GeV. No excess of events is observed at the D_s mass. The resulting limit, calculated using a detection efficiency of 11.2%, the $\eta' \rightarrow \eta\pi^-\pi^+$ and $\eta \rightarrow \gamma\gamma$ branching ratios, and allowing for systematic error (36%) is

$$\frac{\text{B}(D_s \rightarrow \eta'\pi)}{\text{B}(D_s \rightarrow \phi\pi)} < 1.9 \text{ (90\% C.L.)}.$$

The estimate of the systematic error includes the uncertainties in the background shape (25%), in the detection efficiency (26%), and in the integrated luminosity (7.3%).

The Monte Carlo photon efficiency is calibrated using the decay $J/\psi \rightarrow \rho^0\pi^0$. The efficiency for photon detection in the 4.14 GeV data sample is checked using $e^+e^- \rightarrow D^*\bar{D}^*$ events, which are abundant at this center-of-mass energy. A clear $D^0 \rightarrow K^-\rho^+$ signal is observed. The measured ratio, $\text{B}(D^0 \rightarrow K^-\rho^+) / \text{B}(D^0 \rightarrow K^-\pi^+) = 2.5 \pm 0.4$, is in good agreement with the value $2.2_{-0.3}^{+0.4}$ from the Particle Data Group compilation.^[34]

The results on $D_s \rightarrow \eta\pi^+$ are consistent with the measurement $\text{B}(D_s \rightarrow \eta\pi) / \text{B}(D_s \rightarrow \phi\pi^+) \sim 3$ by Mark II^[35] and the limit $\text{B}(D_s \rightarrow \eta\pi^+) / \text{B}(D_s \rightarrow \phi\pi^+) < 1.5$ (90% C.L.) set by E691.^[36] The $\eta'\pi^+$ limit is lower than the ratio $\text{B}(D_s \rightarrow \eta'\pi) / \text{B}(D_s \rightarrow \phi\pi^+) \sim 4.8$ reported by Mark II,^[37] as well as the ratio $\text{B}(D_s \rightarrow \eta'\pi) / \text{B}(D_s \rightarrow \phi\pi) = 6.9 \pm 2.4 \pm 1.4$ reported by NA14'. The results from MARKIII suggest that D_s branching ratios to $\eta\pi$ and $\eta'\pi$ may be much smaller than earlier indications, in agreement with the aforementioned phenomenological models of charm decay.

Summary

A resonant substructure analysis of the mode $D^0 \rightarrow K^- \pi^+ \pi^- \pi^+$ has been performed. A large contribution from the quasi two body pseudoscalar axial vector reaction $D^0 \rightarrow K^- a_1$ is found, in agreement with the prediction of the BSW model. The rate for $D^0 \rightarrow \bar{K}^{*0} \rho^0$ is also measured and found to be smaller than the theoretical expectation. A similar analysis of $D^+ \rightarrow \bar{K}^0 \pi^+ \pi^- \pi^+$ has also been carried out. A large contribution from the quasi two body process $D^+ \rightarrow \bar{K}^0 a_1(1260)^+$ is found in this final state.

Using fully reconstructed candidates for the reaction $e^+ e^- \rightarrow D_s^\pm D_s^{*\mp}$, the model independent limit for the absolute D_s branching fraction $B(D_s \rightarrow \phi \pi^+) < 4.1\%$ is obtained.

A search for the decay modes $D_s \rightarrow \eta \pi$ and $D_s \rightarrow \eta' \pi^+$ is performed. Upper limits for both decay modes are obtained. The branching ratios for these decay modes are much smaller than the branching ratios suggested by earlier measurements from the MarkII and NA14' experiments.

REFERENCES

- 1) $D \rightarrow P P$ will be used as an abbreviation for the decay of a D meson to a pseudoscalar-pseudoscalar final state. Similarly, $D \rightarrow P V$ refers to the decay of a D meson to a pseudoscalar vector final state.
- 2) M.Bauer, B.Stech and M.Wirbel, Z. Phys. C **34**, 103 (1987). Revised values of $a_1 = 1.2$ and $a_2 = -0.5$ are taken from B. Stech, Heidelberg report HD-THEP-87-18, 1987 (unpublished). B.Yu.Blok and M.A. Shifman, Sov. J. Nucl. Phys. **45**, 135 (1987); **45**, 301 (1987); **45**, 522 (1987); **46**, 767 (1987)].
- 3) F. DeJongh, CALT-68-1578. To appear in the Proceedings of the 1989 International Symposium on Heavy Quark Physics, American Institute of Physics.
- 4) We also allow for systematic error in the parameterization of broad resonances and error in the Monte Carlo modeling of the detector.
- 5) This result follows from the isospin decomposition: $A(D^+ \rightarrow K^{*0} \rho^+) = A_{3/2} e^{i\delta_{3/2}}$, $A(D^0 \rightarrow K^{*0} \rho^0) = 1/3(\sqrt{2}A_{3/2} e^{i\delta_{3/2}} - A_{1/2} e^{\delta_{1/2}})$, $A(D^0 \rightarrow K^{*+} \rho^-) = 1/3(A_{3/2} e^{i\delta_{3/2}} + \sqrt{2}A_{1/2} e^{\delta_{1/2}})$
- 6) J.G. Korner and G.R. Goldstein, Phys. Lett. B **89**,105 (1979).
- 7) G.P. Yost et. al. (Particle Data Group), Phys. Lett. B **204**, 1 (1988).
- 8) M.Bauer and B.Stech, Z.Phys.C. 671, 1989.
- 9) For instance, the luminosity required to observe CP violation in the decay $B^0 \rightarrow D^+ D_s^-$ is uncertain by a factor of 2 (in addition to the uncertainty in KM angles and phases) due to the uncertainty in the value of the $B(D_s \rightarrow \phi \pi^+)$.
- 10) J.A. McKenna, Ph.D. thesis, University of Toronto, report RX-1191, 1987.

- 11) G.P. Yost et al. (Particle Data Group), Phys. Lett. B **204**, 1 (1988).
- 12) A. Chen et al., Phys. Rev. Lett. **51**, 634 (1983).
- 13) G. Moneti, in *Proceedings of the XXIII International Conference on High Energy Physics*, Berkeley, 1986, edited by S. Loken (World Publishing, Singapore, 1987).
- 14) M. Althoff et al., Phys. Lett. B **136**, 130 (1984).
- 15) W. Braunschweig et al., Z. Phys. C **35**, 317 (1987).
- 16) H. Albrecht et al., Phys. Lett. B **146**, 111 (1984).
- 17) H. Albrecht et al., Phys. Lett. B **187**, 425 (1987).
- 18) M. Derrick et al., Phys. Rev. Lett. **54**, 2568 (1985).
- 19) S. Abachi et al., Argonne National Laboratory preprint ANL-HEP-CP-86-71, 1986 (unpublished).
- 20) The Particle Data Group's estimate is $B = (8 \pm 5)\%$ (Reference 11).
- 21) W.Y. Chen et al., Phys. Lett. B **226** 192, 1989.
- 22) J. Adler et al., Phys. Rev. Lett. **60** 89, 1988.
- 23) S.R. Wasserbaech, Hadronic Decays of the D_s Meson, SLAC-Report-345, June 1989 and references therein.
- 24) If the unconfirmed modes $D_s \rightarrow \phi \pi^+ \pi^0$ and $D_s \rightarrow K^{*0} K^{*+}$ are omitted from the analysis, the upper limit will increase to 5.9%.
- 25) G. Wormser et al., Phys. Rev. Lett. **61**, 1057 (1988).
- 26) G. Wormser, LAL-89-10 (1989).
- 27) M. Bauer, B. Stech, and M. Wirbel, Z. Phys. C **34**, 103 (1987).
- 28) A. N. Kamal, N. Sinha, and R. Sinha, Phys. Rev. D **38**, 1612 (1988).
- 29) B. Yu. Blok and M. A. Shifman, Sov. J. Nucl. Phys. **45**, 522 (1987).

- 30) A. N. Kamal, N. Sinha, and R. Sinha, Phys. Rev. D **38**, 1612 (1988).
- 31) Phys. Lett. B **222**, 285, 1989 and UCD-88-9.
- 32) S.P.Rosen, Phys. Rev. D **39**, 1349 (1989).
- 33) J. C. Brient, SLAC-PUB-4607, March 1988.
- 34) T. Freese, Ph. D. Thesis, University of Illinois, unpublished (1990).
- 35) The measured cross section times branching fraction at $\sqrt{s} = 29$ GeV is
 $\sigma \cdot B(D_s \rightarrow \eta \pi^+) = 5.2 \pm 2.2$ pb.
- 36) J. C. Anjos et al., Phys. Lett. B **223**, 267 (1989).
- 37) The measured cross section times branching fraction at $\sqrt{s} = 29$ GeV is
 $\sigma \cdot B(D_s \rightarrow \eta' \pi) = 8.4 \pm 3.7$ pb.

The members of the MARK III collaboration are:

G. Dubois, F. DeJongh, G. Eigen, D. Hitlin,

A. Mincer, C. Matthews, W. Wisniewski, Y. Zhu

California Institute of Technology

J. Adler, J.-C. Brient, T. Browder, K. Bunnell,

R. Cassell, D. Coward, C. Grab, P. Kim, J. Labs,

R. Mozley, A. Odian, D. Pitman, R. Schindler,

W. Toki, F. Villa, S. Wasserbaech

Stanford Linear Accelerator Center

Z. Bai, M. Burchell, D. Dorfan, J. Drinkard,

C. Gatto, C. Heusch, W. Lockman,

H. Sadrozinski, M. Scarletella, T. Schalk

A. Seiden, A. Weinstein, S. Weseler

University of California at Santa Cruz

B. Eisenstein, T. Freese, G. Gladding,

J. Izen, A. Wattenberg

University of Illinois, Champaign-Urbana

U. Mallik, M. Roco, M. Wang

University of Iowa, Iowa City

T. Burnett, V. Cook, A. Li, R. Mir,

P. Mockett, B. Nemati, L. Parrish

University of Washington, Seattle

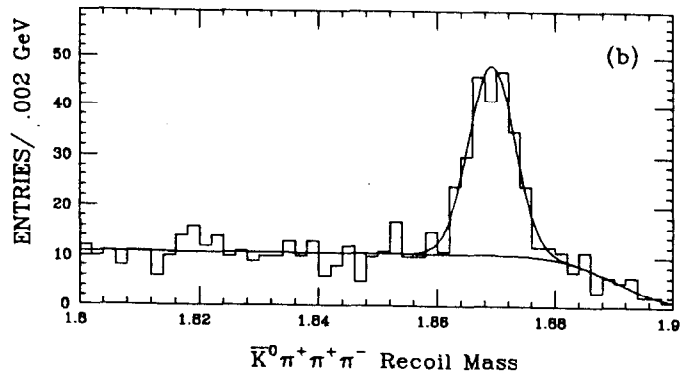
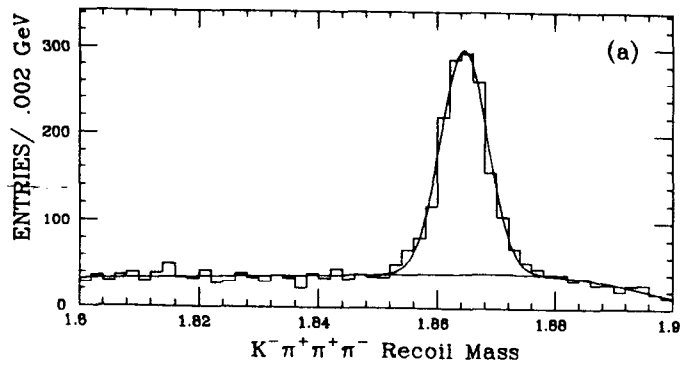


Figure 1. Recoil mass distribution for (a) $D^0 \rightarrow K^- \pi^+ \pi^- \pi^+$ and (b) $D^+ \rightarrow K_s^0 \pi^- \pi^+ \pi^+$

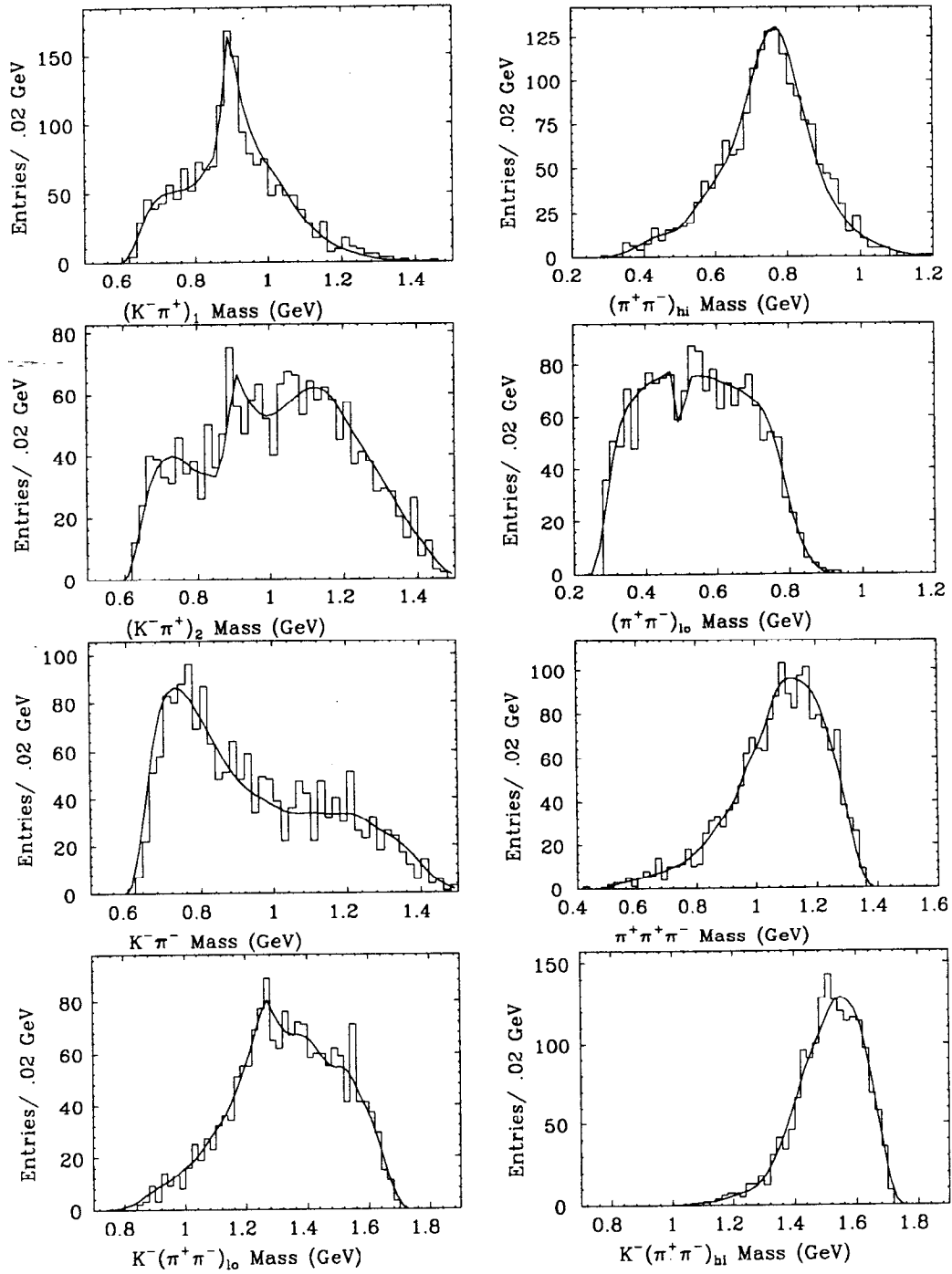


Figure 2. Projections of the likelihood function for $D^0 \rightarrow K^- \pi^+ \pi^+ \pi^-$. The solid lines, representing the projections of the likelihood function, are superimposed on histograms of the events in the signal region. The $\pi^+ \pi^-$ combination with the higher mass is referred to as $(\pi^+ \pi^-)_{hi}$, and the $K^- \pi^+$ combination formed with the π^+ not used in $(\pi^+ \pi^-)_{hi}$ is referred to as $(K^- \pi^+)_1$. The deficit near .5 GeV in the $(\pi^+ \pi^-)_{lo}$ mass plot is due to the rejection of $\pi^+ \pi^-$ combinations which have a high probability of originating from a K_s decay.

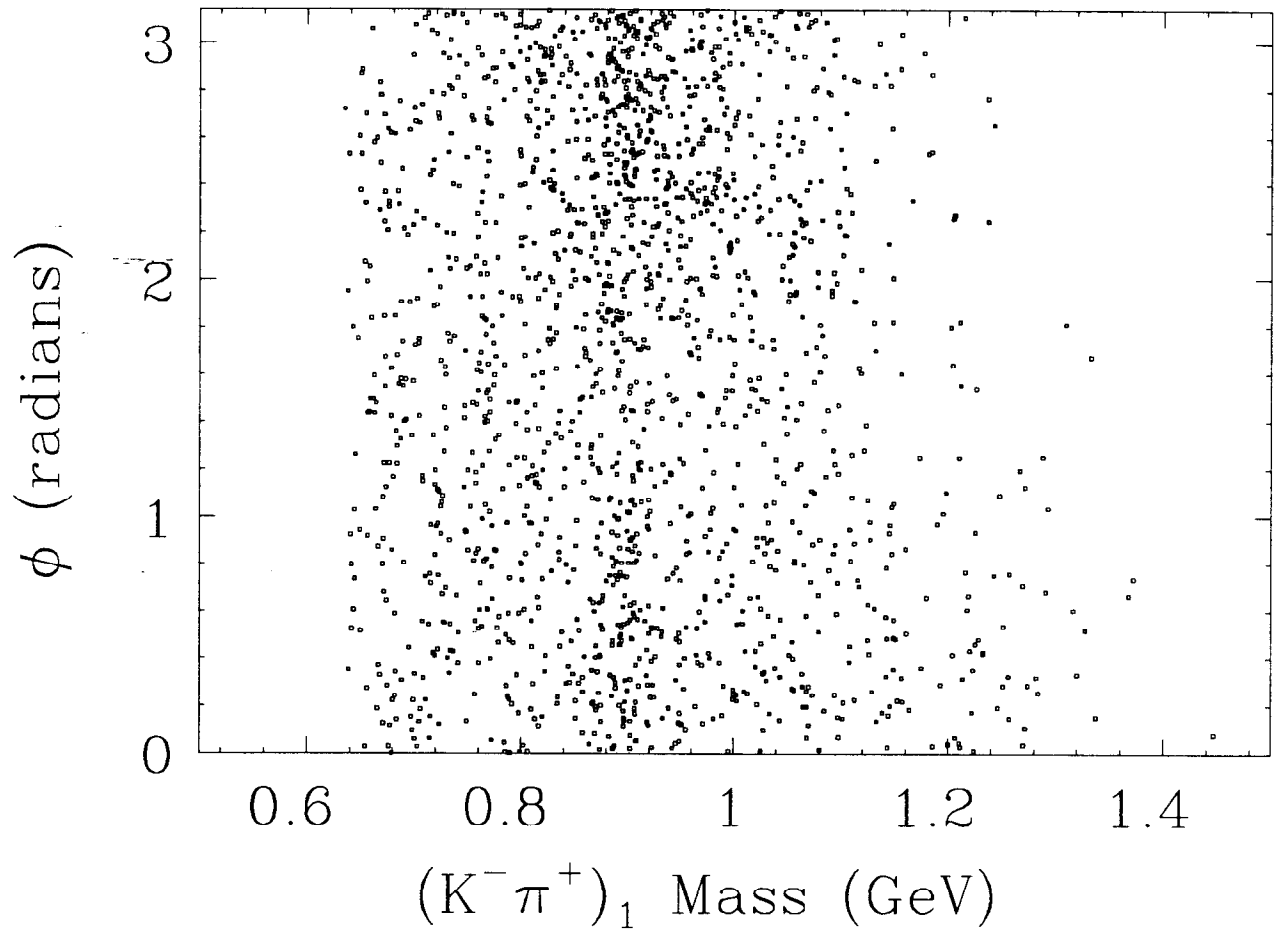


Figure 3. Scatter plot of $(K^- \pi^+)_1$ mass vs ϕ , where ϕ is the angle between the \bar{K}^{*0} and ρ^0 decay planes as seen from the D^0 rest frame. In the \bar{K}^{*0} band, an enhancement near $\phi=0$ and a larger enhancement near $\phi = \pi$ are visible. The transverse $\bar{K}^{*0}\rho^0$ amplitude is proportional to $\cos \phi$ and accounts for this distribution. Since the sign of this amplitude reverses from $\phi = 0$ to $\phi = \pi$, there is more constructive interference near $\phi = \pi$.

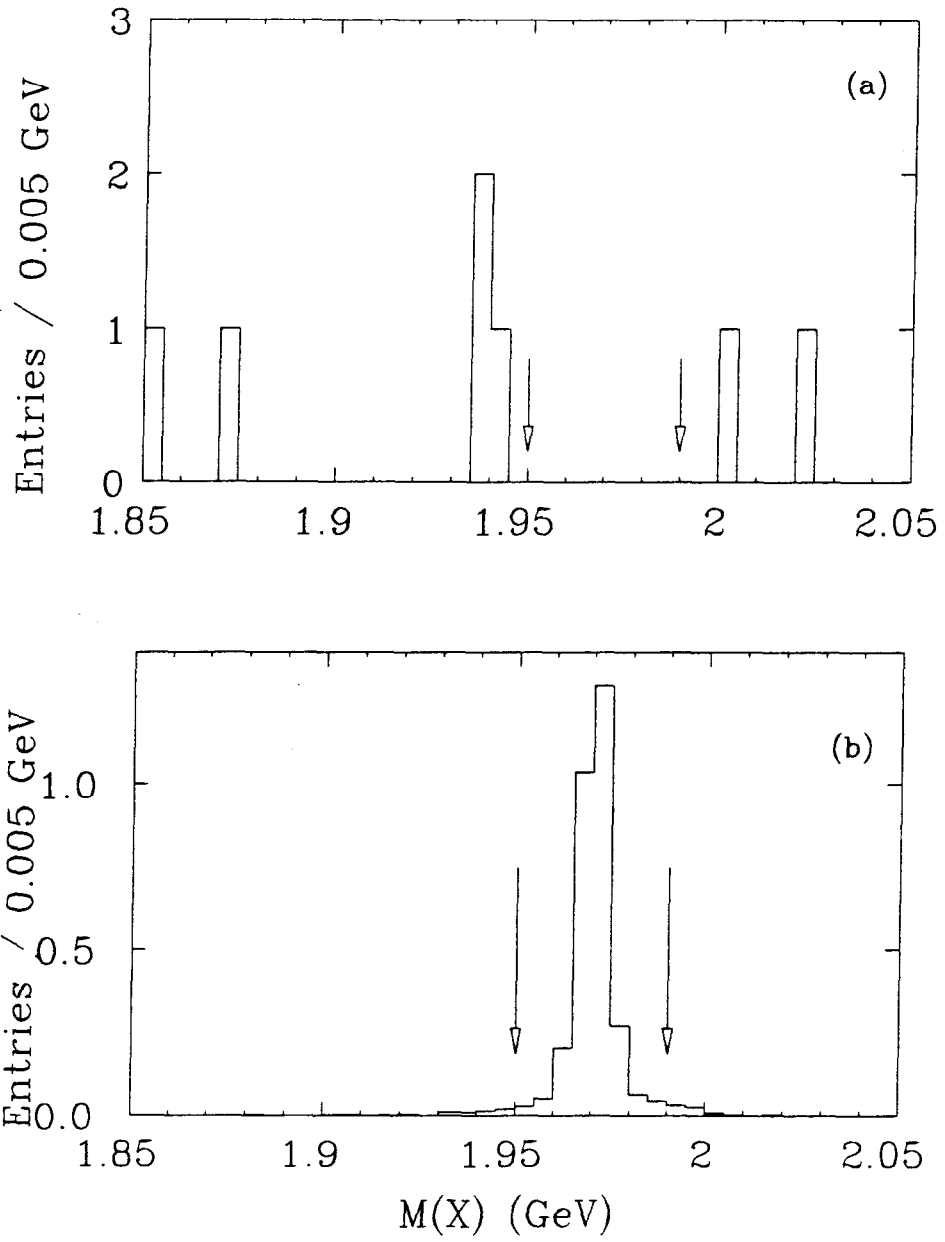


Figure 4. $M(X)$ distribution for (a) data and (b) Monte Carlo events.

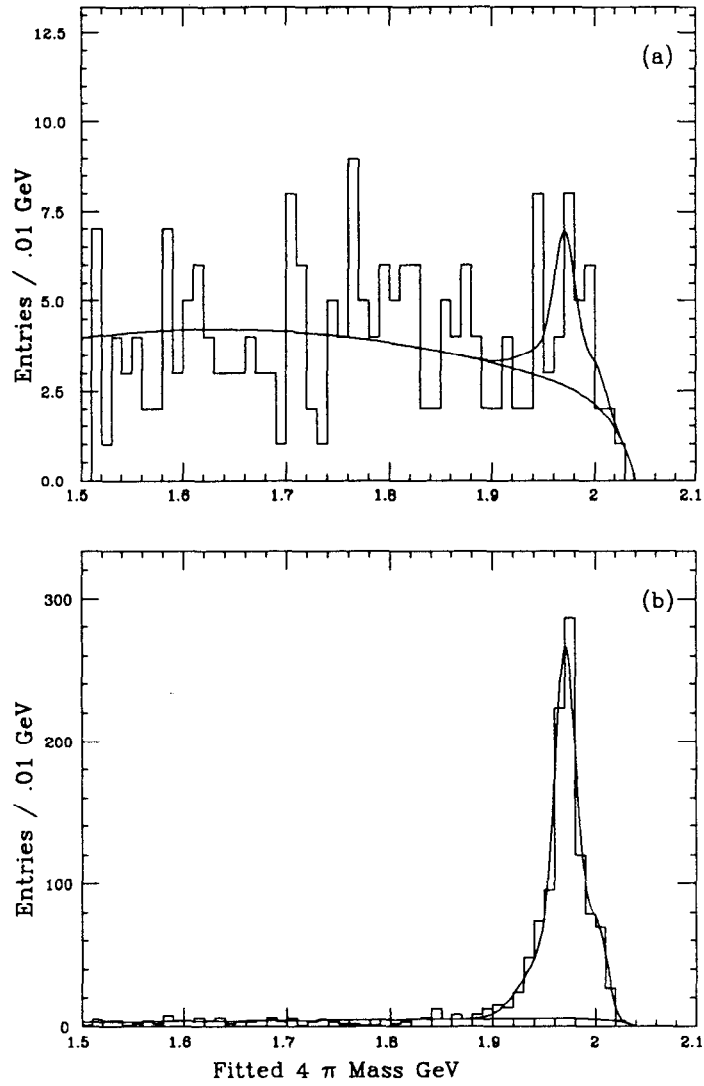


Figure 5. Mass spectrum for $\eta\pi^+$, $\eta \rightarrow \pi^+\pi^-\pi^0$ candidates after 2C kinematic fit: (a) for data events (b) for Monte Carlo events.

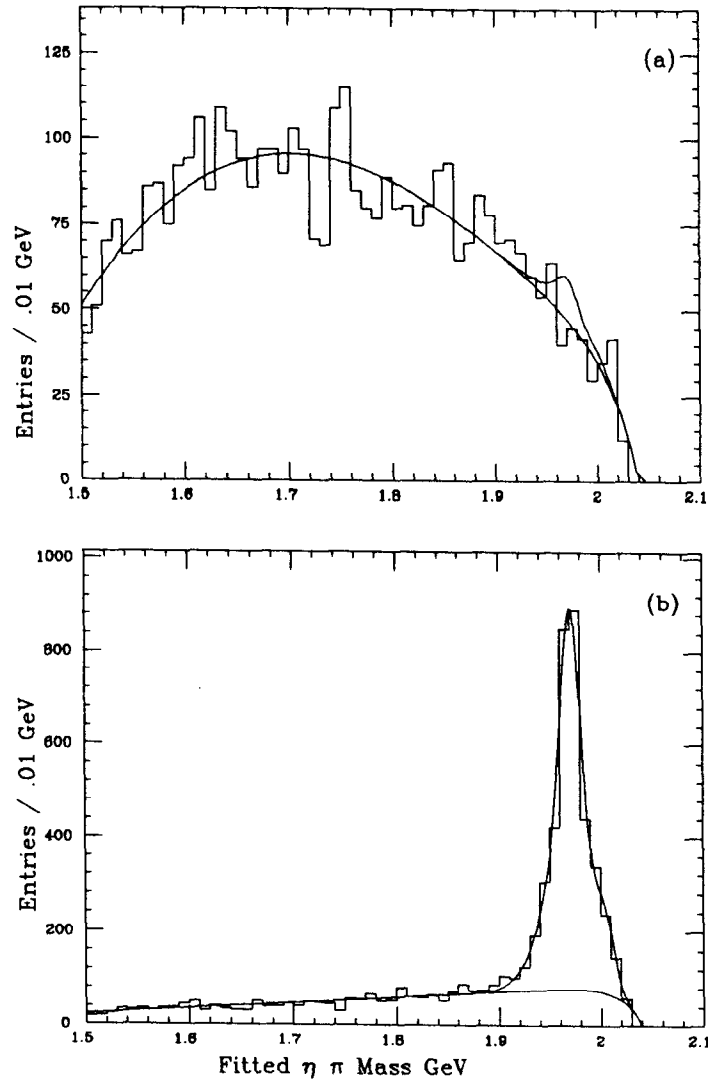


Figure 6. Mass spectrum for $\eta\pi^+$, $\eta \rightarrow \gamma\gamma$ candidates after 2C kinematic fit: (a) for data events (b) for Monte Carlo events.

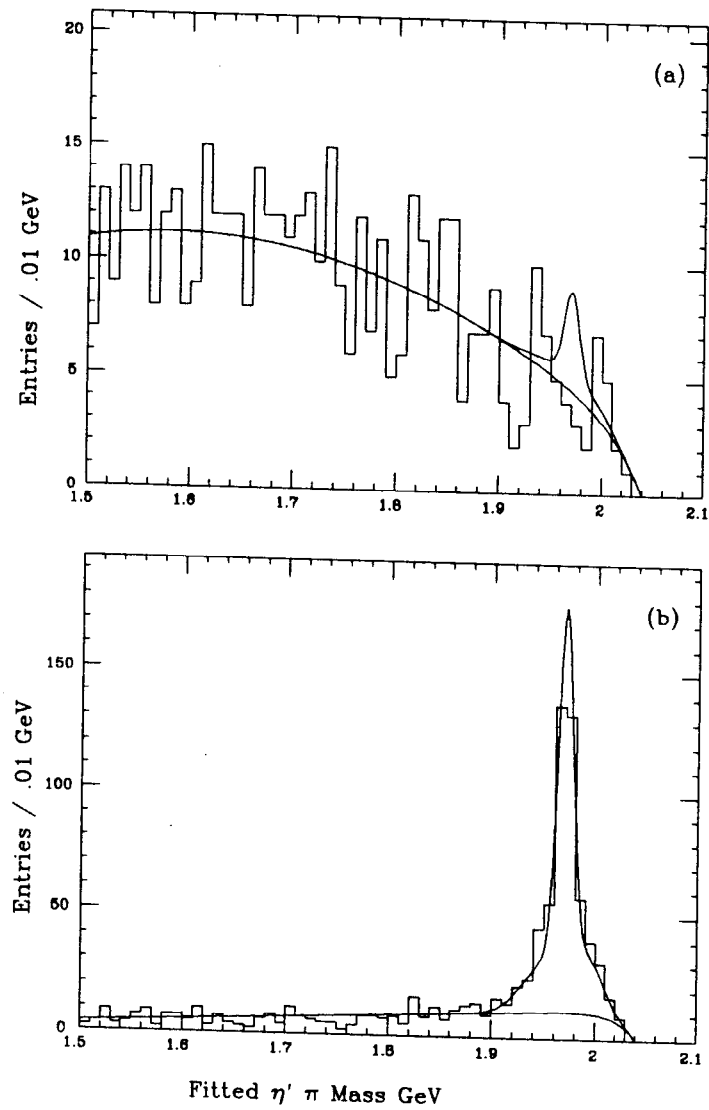


Figure 7. Mass spectrum for $\eta' \pi^+$, $\eta' \rightarrow \eta \pi^+ \pi^-$, $\eta \rightarrow \gamma \gamma$ candidates after 2C kinematic fit: (a) for data events (b) for Monte Carlo events.